Adaptive Vision Localization for Industrial Robots

Teng-Hu Cheng, Yin-Long Yan, Zhe-Hui Chen, Chien-Yu Wu, Shu Huang, and Chin-Chi Hsiao*

***Abstract*—The traditional serial type articulated robot has good positioning repeatability; it is still difficult to have good positioning accuracy. Unfortunately, accuracy is a necessary condition for aviation applications. Under the development of aviation heavy industry, laser tracker is used to promote the accuracy of the robot. However, there are some limitations about using laser odometry in practice: 1. complicated pre-processing and calibration 2. Limited to plain and simple environment 3. Expensive manufacture and maintenance. Therefore, this study developed a visual and inertial system to achieve the objective without less cost. To this end, a light-weight and low-cost visual-inertial localization method is applied to achieve the requirement of the high accuracy of the industry robot. Final, the past two methods and results (Denavit–Hartenberg model calibration and iterative learning control) to improve robot location accuracy are also included in our comparison. The results show that the proposed method has sufficient performance to meet most applications.**

***Index Terms*—robot, localization, adaptive**

Under the demands on energy saving and light-weighted products, aluminum and composite materials have been gradually adopted to replace heavy-weighted steel materials. This change of adoption of raw materials is especially significant for automotive and aerospace industries. In contrast to traditional application specific machinery equipment, industrial robots are more flexible and are more suitable in reconfigurable smart manufacturing system. With the continuous improvement of industrial robot technology, robotic machining will be applied to more machining applications [1].

Industrial robots on flexible and reconfigurable issues, they are appropriate to develop manufacturing systems which are helpful to perform automatically operation such as cutting, drilling, grinding, polishing, milling, and deburring. Industrial robots are applied in the field of aviation manufacturing with the continuous advancement of industrial robot technology. But some problems have also been exposed, such as insufficient accuracy of robots and too many processing points [2]. Therefore, industrial robots need to be more

I. Introduction

The current industrial robots have good repeatability, ranging from ±0.02 to ±0.3 mm. However, in machining applications, it mainly depends on the accuracy of the trajectory accuracy (dynamic/continuous point position) of the industrial robot, instead of the repeatability of the robot. Unfortunately, robot manufacturers usually do not provide accuracy and trajectory accuracy specifications. The accuracy of the robot roughly falls between a few mm to 10 mm [3]. In most manufacturing applications, robot accuracy and trajectory accuracy are prerequisites and mandatory.

We develop a method that fuses visual odometry and a 6-DOF IMU by solving an optimal algorithm, and the estimated robot position is guaranteed by this algorithm. This method can be applied to the machining field or more other related field.

In this study, the accuracy of the robot is corrected by a light-weight and lower-cost positioning equipment. The fusion of the 3D camera and the IMU sensor can improve the average accuracy of robot positioning (≤ 1 mm). In some applications, it can replace the existing high-cost laser positioning correction method. In order to accurately improve the accuracy of the robot, the sampling frequency of the 3D camera must be greater than 100 Hz, and the calibration time must be less than 10 minutes. In addition, the past two methods and results (Denavit–Hartenberg model calibration and iterative learning control, ILC) to improve robot location accuracy are also included in our comparison. Denavit–Hartenberg(D-H) model calibration can decrease the robot location error caused by inaccurate parameters [4, 5]. Iterative learning control consists of an inner loop and an outer loop. Inner loop deals with drive dynamics and outer addresses impreciseness of kinematic parameters as well as joint static bias. hence, iterative Learning Control (ILC) can be used to promote the tracking performance of a robot arm manipulator [6, 7, 8, 9, 10].

The rest of the paper is organized as follows. We briefly describe the ways to improve the accuracy in Section II. The detailed method fusing the measurement data from IMU is described in Section III. The 3D Camera to estimate an optimal

Teng-Hu Cheng received the Ph.D. degree from the Department of Mechanical Engineering, University of Florida, Gainesville, FL, USA, in 2015. In 2016, he joined the Department of Mechanical Engineering, National Yang Ming Chiao Tung University, Hsinchu, Taiwan (e-mail:tenghu@g2.nctu.edu.tw).

Yin-Long Yan received his B.S. from the Department of Mechatronics Engineering at the National Changhua University of Education, Taiwan, in 2019, and is currently a M.S. student in the Dept. of the Graduate Degree Program of Robotics at National Yang Ming Chiao Tung University, Taiwan. (e-mail: yanlong658.gdr08g@nctu.edu.tw).

Zhe-Hui Chen, was with National Chiao Tung University, Hsinchu, Taiwan. He is now with the Department of Mechanical Engineering, National Yang Ming Chiao Tung University. (email: v309611081.en09@nycu.edu.tw)

Chien-Yu Wu is with the Mechanical and Mechatronics Systems Research Laboratories, Industrial Technology Research Institute, Taiwan (e-mail:chienyuwu@itri.org.tw).

Shu Huang is with the Mechanical and Mechatronics Systems Research Laboratories, Industrial Technology Research Institute, Taiwan (e-mail: shu.huang@itri.org.tw).

Chin-Chi Hsiao* is with the Mechanical and Mechatronics Systems Research Laboratories, Industrial Technology Research Institute, Taiwan (886-3-5913896; fax:886-3-5913607; e-mail:hsiao_cc@itri.org.tw). *Corresponding author for this work

position of feature point is described in Section IV. Finally, the experiment results are listed in Section V, followed by a conclusion in Section VI.

II. TECHNICAL GAPS/COMPENSATION METHODS FOR INDUSTRIAL ROBOTS USED IN MACHINING

Basically, there are two methods to improve the accuracy of the robot. The first method is kinematic model correction, and the other is external sensor correction.

A. Kinematic Model Calibration

The economically feasible solution to improve the absolute accuracy of the robot is through the calibration procedure. The method is to identify and compensate the geometric and non-geometric errors in the robot structure. Because these internal errors are usually not easy to measure directly, they must be identified indirectly through attitude errors and the associated mathematical model (DH Model). After constructing the DH Model, the robot is ordered to multiple positions in the workspace, measures the real position and compares the posture error, and then calculates the internal error of the robot structure. After calibration, the error model can be used as a virtual sensor to measure and compensate for robot inaccuracies.

B. External Sensor Correction

Although it is possible to imitate the practice of the automobile industry, manually correct the accuracy with the aid of the teach pendant. However, it is not feasible in practice, because there are huge differences in the number of workpieces and operating procedures. In this case, it is too tedious or even impossible to use manual teaching methods to compensate for robot errors. Therefore, this research focuses on how to feed back the accuracy information of the external sensor (3D camera) to the robot system for further performance improvement.

III. LOW-COST VISUAL LOCALIZATION METHOD

First, define the state of the robot, as in equation (1)

$$\begin{aligned} X &= \left[x_0, x_1, \ldots x_n, x_c^b, \lambda_0, \lambda_1, \ldots \lambda_m\right] \\ x_k &= \left[p_{b_k}^w, v_{b_k}^w, q_{b_k}^w, b_a, b_g\right], k \in [0, n] \\ x_c^b &= \left[p_c^b, q_c^b\right] \end{aligned} \tag{1}$$

Where $x_0, \ldots, x_n$ are states to be estimated. x_k is defined as the state at time t_k. $p_{b_k}^w$, $v_{b_k}^w$ and $q_{b_k}^w$ are respectively the position, speed, and attitude of the arm end-effector at time t_k (world coordinate system). b_a and b_g are the deviation of accelerometer and gyroscope. p_c^b and q_c^b are the relative displacement and relative angle of the camera and the robot.

Second, the optimization problem is expressed as equation (2). The formula is the objective function for minimizing the error between measurement and model. The state function can be solved by nonlinear optimization methods (such as gradient descent method), where $p_{b_k}^w$ and $q_{b_k}^w$ are the optimized arm position and attitude.

$$\min_x \left\{ \begin{array}{c} \left\| r_p - H_p X \right\|^2 + \sum_{k \in B} \left\| r_B\left(\hat{z}_{b_{k+1}}^{b_k}, x\right) \right\|_{P_{b_{k+1}}^{b_k}}^2 + \\ \sum_{(i,j) \in B} p\left(\left\| r_C(\hat{z}_l^{cj}, x) \right\|_{P_l^{cj}}^2 \right) \end{array} \right\} \tag{2}$$

$r_B\left(\hat{z}_{b_{k+1}}^{b_k}, x\right)$ and $r_C\left(\hat{z}_l^{cj}, x\right)$ are residuals for IMU and visual measurements respectively. Detailed definition of the residual terms will be presented in equation (3) and equation (4). B is the set of all IMU measurements, C is the set of features which have been observed at least twice in the current sliding window. $\{r_p, H_p\}$ is the prior information from marginalization.

The first term in equation (2) is initialization, and the second term is the error generated by the displacement integral of the IMU and the motion model, as in equation (3).

$$\begin{aligned} r_B(\hat{z}_{b_{k+1}}^{b_k}, x) &= \begin{bmatrix} \delta\alpha_{b_{k+1}}^{b_k} \\ \delta\beta_{b_{k+1}}^{b_k} \\ \delta\theta_{b_{k+1}}^{b_k} \\ \delta b_a \\ \delta b_g \end{bmatrix} \\ &= \begin{bmatrix} R_w^{b_k}\left(p_{b_{k+1}}^w - p_{b_k}^w + \frac{1}{2} g^w \Delta t_k^2 - v_{b_k}^w \Delta t_k\right) - \hat{\alpha}_{b_{k+1}}^{b_k} \\ R_w^{b_k}\left(v_{b_{k+1}}^w + g^w \Delta t_k - v_{b_k}^w\right) - \hat{\beta}_{b_{k+1}}^{b_k} \\ 2\left[\left(q_{b_k}^w\right)^{-1} \otimes q_{b_{k+1}}^w \otimes \left(\hat{\gamma}_{b_{k+1}}^{b_k}\right)^{-1}\right]_{xyz} \\ b_{ab_{k+1}} - b_{ab_k} \\ b_{\omega b_{k+1}} - b_{\omega b_k} \end{bmatrix} \end{aligned} \tag{3}$$

where $[.]_{xyz}$ extracts the vector part of a quaternion q for error state representation, and $\otimes$ denotes the multiplication for quaternions (i.e., Hamilton product), and $\delta\theta_{b_{k+1}}^{b_k}$ is the three-dimensional error-state representation of quaternion. [$\hat{\alpha}_{b_{k+1}}^{b_k}$, $\hat{\beta}_{b_{k+1}}^{b_k}$, $\hat{\gamma}_{b_{k+1}}^{b_k}$] are pre-integrated IMU measurement terms using only noisy accelerometer and gyroscope measurements within the time interval between two consecutive image frames. The accelerometer and gyroscope biases are also included in the residual terms for online correction.

The third term is the error produced by the camera measurement and the state estimation model to correct the actual displacement, as shown in equation (4). Although the integration of the second term will cause the error to accumulate, the error can be corrected back through the third formula.

$$\begin{aligned} r_c(\hat{z}_l^{cj}, x) &= [b_1 \quad b_2]^T \bullet \left(\hat{\bar{P}}_l^{cj} - \frac{P_l^{cj}}{\left\| P_l^{cj} \right\|}\right) \\ \hat{\bar{P}}_l^{cj} &= \pi_c^{-1}\left(\begin{bmatrix} \hat{u}_l^{cj} \\ \hat{v}_l^{cj} \end{bmatrix}\right) \end{aligned} \tag{4}$$

Where [$\hat{u}_l^{cj}$, $\hat{v}_l^{cj}$] is the observation of the same feature in the

j -th image. π_c^{-1} is the back projection function which transforms a pixel location into a unit vector using camera intrinsic parameters. Since the degrees-of-freedom of the vision residual is two, we project the residual vector onto the tangent plane. b1, b2 are two arbitrarily selected orthogonal bases that span the tangent plane of $\hat{\hat{P}}_l^{c_j}$.

$$\min_x \left\{ \begin{array}{l} \left\| r_p - H_p X \right\|^2 + \sum_{k \in B} \left\| r_B \left(\hat{z}_{b_{k+1}}^{b_k}, x \right) \right\|_{P_{b_{k+1}}^{b_k}}^2 + \\ \sum_{(i,j) \in B} p \left(\left\| r_C \left(\hat{z}_l^{cj}, x \right) \right\|_{P_{P_l}^{c_j}}^2 \right) \end{array} \right\} \quad (5)$$

Finally, $p_{b_k}^w$ can be used to compute the error with the ground truth to evaluate the accuracy.

IV. VISION SERVO SYSTEM CALIBRATION

A. *Camera coordinate system and image coordinate system*

In order to understand the relationship between 2D image and 3D relative distance, it is necessary to understand the relationship between the camera coordinate system and the image coordinate system. Figure 1 is a schematic diagram of camera coordinates and image coordinates. P(X,Y,Z) is a point in the three-dimensional space observed in the camera coordinate system. The corresponding point where P is projected onto the image plane is $P_j(u, v)$.

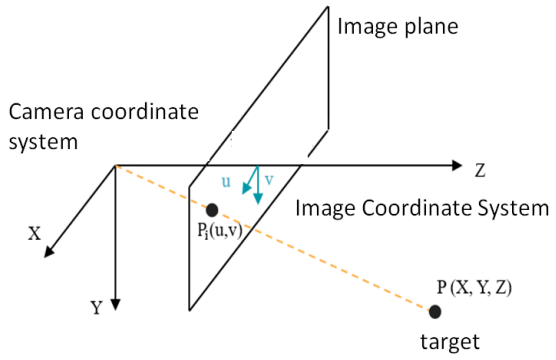

Figure 1. schematic diagram of camera coordinates and image coordinates.

In general, the origin of the image coordinate is the upper left corner of the image plane, so there is a translational relationship between the camera coordinate system and the image coordinate system as shown in Figure 2.

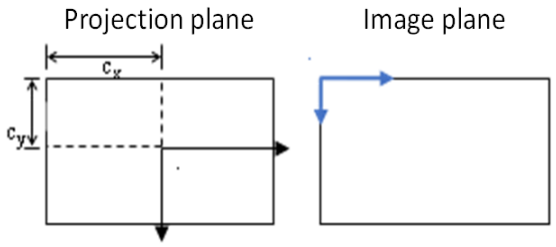

Figure 2. Schematic diagram of projection plane and image plane coordinates

Let $f_x$and f_y be the focal lengths in the X-axis and Y-axis directions respectively, and a homogeneous matrix can be produced.

$$\begin{bmatrix} u \\ v \\ w \end{bmatrix} = \begin{bmatrix} f_x & 0 & c_x \\ 0 & f_y & c_y \\ 0 & 0 & 1 \end{bmatrix} \begin{bmatrix} X \\ y \\ Z \end{bmatrix}$$

$$\text{where } (u, v, w) = \left(\frac{f_x}{Z} + c_x, \frac{f_y}{Z} + c_y, 1 \right)$$

B. *Camera calibration*

In order to correctly estimate the actual distance of the target object, the internal parameters of the camera f_x, f_y, c_x, and c_y need to be obtained first. Camera calibration can calculate the camera's internal parameter matrix (Intrinsic Matrix) and external parameter matrix (Extrinsic Matrix). The internal parameters can be obtained f_x, f_y, c_x, and c_y. The external parameters can obtain the rotation matrix of the camera relative to the world coordinate (including translation and rotation). Pinhole Camera Model can be expressed as follows:

$$s \begin{bmatrix} u \\ v \\ 1 \end{bmatrix} = \begin{bmatrix} f_x & 0 & c_x \\ 0 & f_y & c_y \\ 0 & 0 & 1 \end{bmatrix} \begin{bmatrix} r_{11} & r_{12} & r_{13} & t_1 \\ r_{21} & r_{22} & r_{23} & t_2 \\ r_{31} & r_{32} & r_{33} & t_3 \end{bmatrix} \begin{bmatrix} x \\ y \\ x \\ 1 \end{bmatrix}$$

When the focal length of the camera is fixed, the internal parameter matrix will not change with the movement of the object or the movement of the camera. From these data, the required image characteristics can be further obtained. Camera calibration package provided by ROS is used to calibrate the camera. Detailed calibration information is based on [11, 12].

C. *Image positioning*

According to [13], the positioning system can be completed through a 3D camera and an inertial measurement system (IMU). In this system, the IMU and camera are fixed on the robot, as shown in Figure 3. As the robot moves, the actual position, distance and posture of the movement can be detected to provide information for assisting positioning. In this system, the distance of movement can be estimated through the feature points in the environment. In practice, artificial feature points (such as Apriltag) can be used to increase reliability. The fusion of the two sensors makes a higher positioning accuracy through the measurement of the camera's Odometry and IMU.

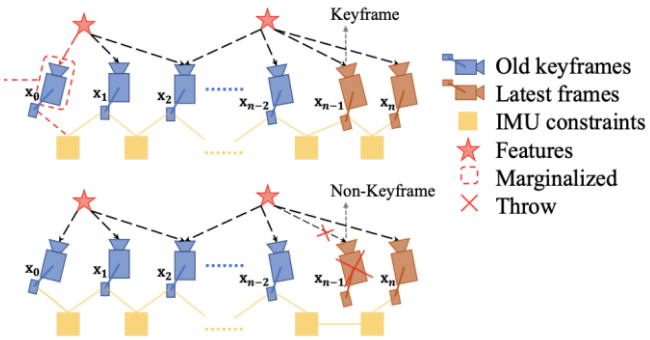

Figure 3. Visual inertia Odometry.

V. Experimental Result

A. *Experimental result*

In the experiment, a reflective ball and Laser Photosphere position will be installed on the robot, as shown in Figure 4. The high-speed camera positioning system is used to locate the end-effector of the robot, and the laser tracker is used for measurement at the same time. The measured value of the Laser tracker can be used as ground truth to obtain the error. Figure 5 shows the setup of the 3D camera.

In addition, the past two methods (Denavit–Hartenberg model calibration and iterative learning control) to improve robot location accuracy are also included in our comparison. Section B shows the results of the Denavit–Hartenberg model calibration. Section C shows the results of the iterative learning control. Different from the 3D camera used in this research, both methods use Laser tracker as the robot position measurement tool. Table I shows the specification of the 3D camera and Laser tracker. Although the laser tracker has excellent measurement capabilities, the high price hinders its popularity.

Figure 4. experiment setup: robot and reflective ball.

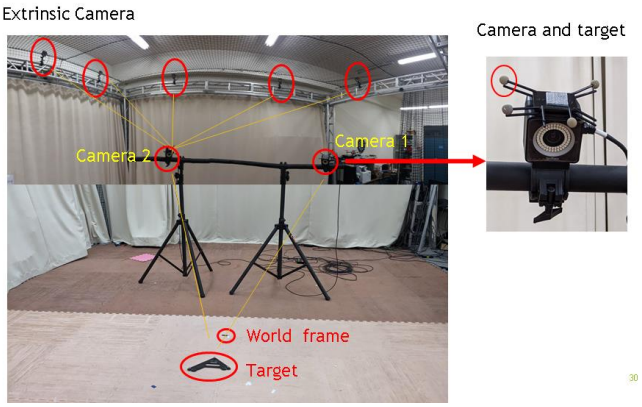

Figure 5. experiment setup: Camera.

Table I. Specification: 3D camera vs Laser tracker

Specification	3D camera	Laser tracker
Brand	Optitrack	Leica
Measurement volume	FOV:82°×70° 240 Frame/sec Resolution:1280×1024	160 m horizontal :360° vertical: ±45°
Measuring precision	<0.3 mm	15 μm + 6 μm/m
cost	$ 27,000	$ 200,000

Since the coordinate systems of the two sensors are different, and the laser tracker lacks a posture measurement function. Therefore, the experimental design is to give 10 way points on a straight line trajectory, and stay on them for a while, and finally compare the position errors of the 10 way points, as shown in Figure 6. The reason of using this method is that a transformation between the frames of the two sensors through the 10 waypoints can be constructed. Table II shows the results of 9 experiments, the average error is about 0.53mm.

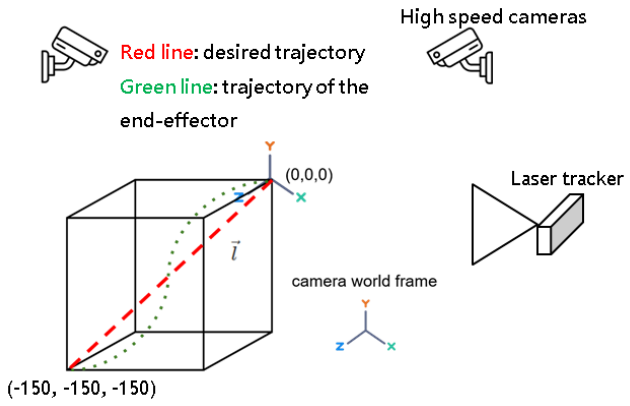

Figure 6. Experiment description.

Table II. Experimental Statistics for 3D vision calibration

No. of experiment	Real distance (mm)	Measured distance (mm)	Absolute error (mm)	Error (%)
1	20	18.33	1.67	8.35

2	20	19.96	0.04	0.2
3	20	18.40	1.6	8
4	20	20.10	0.10	0.5
5	20	20.26	0.26	1.3
6	20	19.41	0.59	2.95
7	20	19.88	0.12	0.6
8	20	19.15	0.85	4.25
9	20	19.74	0.26	1.3
Ave.	20	19.47	0.53	2.65

B. Compared with Denavit–Hartenberg Model Calibration

The economically feasible solution to improve the absolute accuracy of the robot is to identify and compensate the geometric and non-geometric errors in the robot structure. Because these internal errors are usually not easy to measure directly, they must be identified indirectly through attitude errors and the associated mathematical model (D-H Model). After constructing the model, the robot is ordered to multiple positions in the workspace, the actual position is actually measured and the attitude error is compared, and then the internal error of the robot structure is calculated. After calibration, the error model can be used as a virtual sensor to measure and compensate for robot location.

Figure 7 shows the setup of the robot and laser tracker for D-H model calibration. In the calibration process, 100 points of information are used for D-H model parameter correction. Table III shows that the max error is about 0.42 mm and RMS error is about 0.10 mm.

Figure 7. experiment setup: robot and laser tracker.

Table III. Experimental Statistics for D-H model calibration

	X	Y	Z	Total
Max error (mm)	0.14	0.34	0.2	0.42
RMS error (mm)	0.05	0.06	0.07	0.10

C. Compared with Iterative Learning Control Compensation

ILC is a relatively a new technique. It ccan used to improving the transient response and tracking performance of any physical system. It is a technique for systems with repetitive operations, which are modified based on the observed error to control the input signal at each repetitive operation. By the error in the output response after each operation and using the error to fix the input signal to the system, ILC can improve the system performance [14]. Hence, it suits to robot that is required to execute a particular operation repeatedly.

Table IV shows that the max error is about 1.244 mm and RMS error is about 0.816 mm without ILC compensation or D-H model calibration. Under the condition of ILC compensation, the max error is about 0.511 mm and RMS error is about 0.195 mm. In other words, ILC has a performance improvement of more than 2 times.

Table IV. Experimental Statistics for ILC Compensation

Test Conditions	RMS Error / Max Error
without ILC	0.816 / 1.244
with ILC	0.195 / 0.511

The DH model correction technique has the best results. The results of the ILC technology are slightly better than the results of the 3D camera compensation technology, but this does not mean that the method proposed is not good. The main reason is the obvious performance difference between the 3D camera and the Laser tracker. If the 3D camera can have better performance, the accuracy of the robot can be significantly improved. Even so, the proposed method has sufficient performance to satisfy most applications. In addition, D-H model calibration combined with ILC or the vision compensation technology proposed in this research can achieve better results.

VI. CONCLUSION

The estimation algorithms and optimization algorithms are used to enable the robot to ensure high-precision positioning through the calibration of measuring instruments (general accuracy). According to the experimental results, the average error after correction is 0.53 mm. Compared with the past two methods and results of using Laser tracker to improve robot accuracy (D-H model calibration 0.36 mm and iterative learning control 0.511 mm), the proposed method has sufficient performance to meet most applications. After many tests, the positioning error is within 8%, and the repeatability of the proposed method is acceptable. By reducing environmental interference and correcting the internal parameters of the 3D camera, the repeatability can be improved. Once the repeatability can be reduced, there is an opportunity to establish a compensation model to reduce the positioning error.

In terms of cost analysis, the visual sensor fusion method can reduce costs compared to the laser tracker solution. At the same time, the pre-positioning work can be simplified, and there is no need to spend time installing too many large instruments. Through the trajectory of the robot and the real-time positioning of this method, it can be inferred which angle of the robot will cause a large positioning error. In the future, the cause of the problem can be analyzed (e.g., motor, reduction mechanism, and

controller). In this study, 3D vision is used to assist the positioning of the robot. In addition to improving the positioning accuracy of the robot. In the future, sensors can be combined with automatic calibration to reduce manpower requirements and gradually develop towards Industry 4.0.

ACKNOWLEDGMENT

Thanks to the support of the Department of Industrial Technology (Project Number:L353C80000), so that this research can be carried out smoothly.

REFERENCES

[1] I. Iglesias, M.A. Sebastián, J.E. Ares, "Overview of the state of robotic machining: Current situation and future potential", *The Manufacturing Engineering Society International Conference, Procedia Engineering*, vol. 132, p911-917, 2015.
[2] Brian Rooks,"Automatic wing box assembly developments", *Industrial Robot: An International Journal*, vol. 28 no, 4, pp.297- 302, 2001.
[3] Siciliano, B., Khatib, O., Handbook of Robotics, Springer, 2008.
[4] M. Abderrahim, A.Khamis, S.Garrido,and L.Moreno," Accuracy and calibration issues of industrial manipulators," *Industrial Robotics: Programming, Simulation and Applications*, pp. 131-146, 2006.
[5] Mohamed Abderrahim, Alla Khamis, Santiago Garrido, and Luis Moreno," *Accuracy and Calibration Issues of Industrial Manipulators," Industrial Robotics - Programming, Simulation and Applications*, pp. 131-146, December, 2006.
[6] C. W. Chen and T. C. Tsao," Data-driven progres-sive and iterative learning control," *IFAC-PapersOnLine*, vol .50, no. 1, pp. 4825–4830, 2017.
[7] Y. M. Zhao, Y. Lin, F. Xi, and S. Guo," Calibration-based iterative learning control for path tracking of industrial robots," *IEEE Transactions on industrial electronics*, vol. 62, no. 5, pp. 2921–2929, 2015.
[8] K. T. Teng and T. C. Tsao," A comparison of inversion based iterative learning control algorithms," *In American Control Conference (ACC)*, pp. 3564–3569, 2015.
[9] C. Wang, M. Zheng, Z. Wang, C. Peng, and M. Tomizuka," Robust iterative learning control for vibration suppression of industrial robot manipulators," *Journal of Dynamic and Systems, Measurement, and Control*, vol. 140, no. 1, 2018.
[10] V. Zundert J and T. Oomen," On inversion-based approaches for feedforward and ILC," *Mechatronics*, vol. 50, pp. 282-291, 2018.
[11] Camera Calibration, http://wiki.ros.org/camera_calibration
[12] Camera Calibration With OpenCV, https://docs.opencv.org/2.4/doc/tutorials/calib3d/camera_calibration/camera_calibration.html
[13] T. Qin, P. Li, and S. Shen, "VINS-Mono: A Robust and Versatile Monocular Visual-Inertial State Estimator," *IEEE Transactions on Robotics*, vol. 34, no. 4, pp. 1004-1020, 2018.
[14] Y. H. Lee, S. C. Hsu, T. Y. Chi, Y. Y. Du, J. S. Hu, and T. C. Tsao," Industrial robot accurate trajectory generation by nested loop iterative learning control," *Mechatronics*, vol. 74, 2021.

Teng-Hu Cheng received the M.S. degree in Department of Mechanical Engineering from National Taiwan University, Taiwan, in 2009, and Ph.D. degree in Department of Mechanical Engineering from University of Florida, Gainesville, FL, USA, in 2015. He is currently a associate professor with the Department of Mechanical Engineering, National Yang Ming Chiao Tung University, Taiwan. His current research interests and publications are in the areas of UAV and Robotics.

Yin-Long Yan will receive the M.S. degree in Department of Mechanical Engineering from National Yang Ming Chiao Tung University, Taiwan, in 2021.

Zhe-Hui Chen will receive the M.S. degree in Department of Mechanical Engineering from National Yang Ming Chiao Tung University, in 2022.

Chien-Yu Wu received the M.S. degree in Departments of Computer Science and Information Engineering from Chung Hua University, Taiwan, in 2005, and Ph.D. degree in Departments of Computer Science and Information Engineering from National Chung Cheng University, Taiwan, in 2014. He is currently a Deputy Manager with the Industrial Technology Research Institute, Taiwan. His current research interests and publications are in the areas of robotics and motion control.

Shu Huang received the M.S. degree in Department of Mechanical Engineering from National Chiao Tung University, Taiwan, in 1999, and Ph.D. degree in Department of Mechanical Engineering from University of Leuven, Belgium, in 2011. He is currently the Director of Intelligent Robotics Division in Industrial Technology Research Institute, Taiwan, as well as an Adjunct Assistant Professor in NYCU, Taiwan. His current research interests are in the areas of robotics, advanced motion planning, CPS system, medical robotics, and bio-inspired behavior-based mobile manipulation.

Chin-Chi Hsiao received the M.S. degree in Department of Mechanical Engineering from Chung Yuan Christian University, Taiwan, in 2000, and Ph.D. degree in Department of Mechanical Engineering from National Chiao Tung University, Taiwan, in 2007. He is currently a researcher with the Industrial Technology Research Institute, Taiwan. His current research interests and publications are in the areas of service and industry robot.